Fachtagung "Experimentelle Strömungsmechanik"
3. – 5. September 2019, Erlangen

Einfluss konvexer, strukturierter Oberflächen auf turbulente Kanalströmungen bei unterschiedlichen Kanalhöhen.

Influence of convex structured surfaces on turbulent channel flow at different channel heights.

Mohamed Yousry, Sebastian Merbold, Christoph Egbers.
Brandenburg University of Technology Cottbus-Senftenberg, Dept. Aerodynamics and Fluid Mechanics, Siemens-Halske-Ring 14, D-03046 Cottbus, Germany

Schlagworte : Hexagonale Strukturen; Geschwindigkeitskontur ; LDA Messungen.
Key words : Hexagonal Structures; velocity contour; LDA Measurements

Abstract

Arrays of convex hexagonal structured with height (k) to diameter (D) ratio is 86% are studied in a turbulent channel flow at Reynolds numbers between 10900 and 38 000. Two different channel heights (H) 20, and 50 mm were tested, i.e., the ratios of the channel full height (H) to structure height (H/k) were chosen to be 6.4, and 16.1 respectively.

LDA measurements were conducted to measure the stream wise and wall normal velocity components. For computing the mean velocity of the local flow measurements at least 20000 samples were acquired at every measuring position. Also LDA measurements over the horizontal x-z plane have been measured starting from y/H = 0.05 to the channel centerline at y/H = 0.5 within the hexagonal structured cavity depression inside turbulent channel flow. These measurements were carried out with a relatively coarse measurement grid spacing with $\Delta x \approx 0.07D$ and $\Delta z \approx 0.07D$ above the hexagonal structured cavity, where D is the diameter of hexagonal structured cavity. All LDA measurements have been measured with the origin (x = 0, z = 0) centered at the center hexagonal structured cavity of the 11th row of the structured array as shown in fig.(1), to insure that the flow reached the equilibrium state. Pressure gradients were calculated from static pressure measurements using 16 pressure taps along the channel to capture the effect of the convex hexagonal structures on drag in the channel flow.

The present investigation is studying the influence of the H/k on the turbulent flow properties inside a convex hexagonal structures (CS) of channel compared with the smooth plain (SPS) turbulent channel flow and reveal the flow behaviour around a single hexagonal structured cavity.

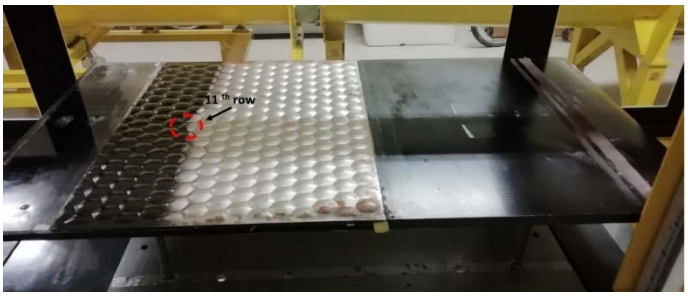

Fig. 1: Structured sheet plate fixed over the lower flat plate. Second plate is mounted above with a separation distances.

Introduction

In the last two decades, there was an increasing of interest in using structured surfaces such as dimples with the aim of reducing the turbulent drag. Early efforts as in the experimental study of (Alekseev et al. 1998) reported significant drag reduction of up to 20% for dimpled surfaces compared with the flat surfaces. However, more recent work like that of (Lienhart et al. 2008), who combined both experimental and numerical studies, reports only small or no drag reduction for dimples in both open and internal boundary layers. No clear reason has been found for the conflict in such results, and on the top that the many parameters that affect the flow over dimples add much to the overall confusion. This is particularly due to the fact that many of these parameters, such as the flow turbulence intensity, are often unreported. The flow structure over the dimples is influenced differently by a various structure geometry and flow parameters.

One of the most significant parameters is the dimple depth, which is often non-dimensionalized by the dimple diameter. The effect of ratio of the dimple depth to diameter has been studied extensively in experiments by (Burgess et al. 2005, Ligrani et al. 2001, Merbold 2009) and numerically by (Isaev et al. 2003, Wang et al. 2006). Flow visualizations (Kovaleko et al. 2010, Kwon et al. 2011, Tay et al. 2014) have shown that when ratio of dimples depth to diameter is greater than 10% generation of vertical and streamwise vortices takes place. These vortices, which are sometimes periodic, greatly increase the mixing within the flow. The majority of these studies involve dimples in an internal flow environment such as in a channel or pipe. Numerous empirical relations have been proposed relating to useful parameters such as friction factors with the dimple depth to diameter ratio, Reynolds number, inlet turbulence intensity, channel height, and even the channel aspect ratio (Mahmood et al. 2002, Ligrani et al. 2005, Isaev et al. 2010).

In a study by (Butt et. al. 2013 and 2016), investigations have been performed on the flow over a hexagonal structured surfaces including hexagonal structured cylinders, hexagonal structured plates and hexagonal structure turbine blades. It was reported that the drag coefficient of the structured cylinder with convex hexagonal patterns were observed to be lower than the smooth cylinder by 65% .While for the flat plate [fig (2)], the maximum reduction in shear stress coefficient was recorded for concave structured surface of about 19% compared to the smooth surface (Butt et al.2014). The present study focuses on the effect of the flow behaviour around a single hexagonal structured cavity and discuss the impact of the structured surface onto the flow.

Experimental Setup

The experimental investigation for the channel flow is conducted for Reynolds number $Re = U_b\, d / v = 10900$ (using bulk velocity U_b, channel half-width $d = h/2$) in wind tunnel of the aerodynamics and fluid mechanics department as shown in fig.(2). The wind tunnel, Göttingen type, was equipped with a cooling system to fix the temperature at 20 ºC. Two Plexiglas plates spanning the whole length of the channel were used as side walls to allow optical access of the flow. Three strips of tripping device sandpapers were used to trigger the turbulent boundary layer at x/D=0 as in fig (1) to insure that the flow is fully turbulent. The Upper and lower plates are equipped with a wide pocket served as a platform for the structured sheets to be investigated. The test sheets of similar width of the upper and lower plates and smaller in length were placed in the pocket of the plates and fixed with the help of fixing elements on both sides. The surface of the test sheet was setting flush to the surface of the plates to avoid stepping and

GALA e.V., Karlsruhe, Germany, ISBN 978-3-9816764-6-4

hence any local separation of the flow as shown in fig.(1). The characteristic dimensions of the channel is 11.9 and 22.4 spanwise and streamwise respectively. For Channels having high aspect ratio (W/D ≥ 10), the side wall effects on the core flow structure can neglected. (Marusic et al. 2010)

For better understand the mechanism and reason for the observed drag reduction, further measurements were taken at very high spatial resolution with $\Delta x \approx 0.07D$ and $\Delta z \approx 0.07D$ above the hexagonal structured cavity, double that for the measurements at four different heights at y/H = 0.5, 0.25, 0.125, and 0.05.

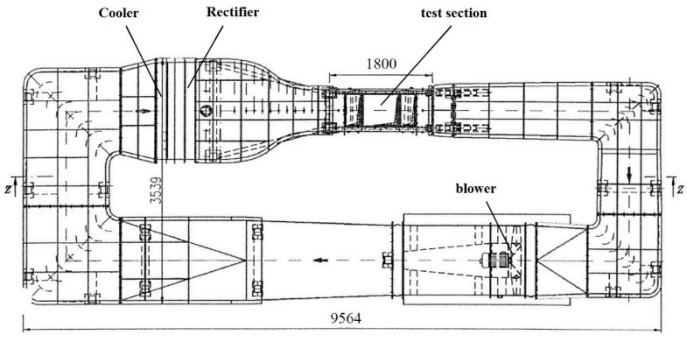

Fig. 2: Gottingen wind type tunnel at LAS.

Measurement techniques

I- Laser Doppler Anemometry (LDA)

All LDA measurements have been conducted over convex hexagonal structured cavity at the 11th row of the tested sheet using two dimensional Laser-Doppler anemometry. The focal length of the LDA during the measurements was 310 mm and the measuring volume was 45 µm. For computing the mean velocity of the local flow measurements at least 20000 samples were acquired at every measuring position. A computer controlled three dimensional high spatial resolution traverse system (Isel Germany AG) was in use for traversing the laser doppler anemometry probe. The traverse is placed on scaled rail to facilitate its movement in streamwise, spanwise, and normalwise directions. The minimum step with the traverse mechanism is 6,35 µm.

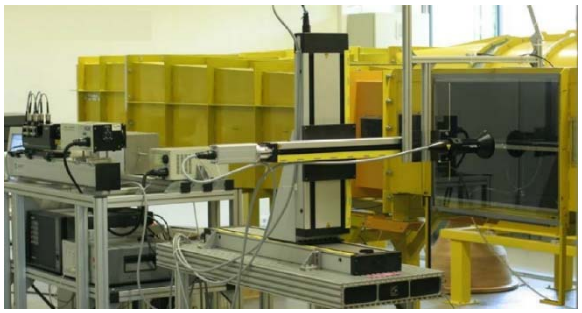
Fig. 3: LDA measurement experimental setup.

II- Particle Image Velocimetry (PIV)

Particle Image Velocimetry (PIV) measurements have been carried out rear the tested sheets. A standard Nd: YLF double-pulse laser, having 527nm/pulse was utilized. The measurements were carried out using CMOS camera, having 2560×1600 pixels, was installed with sampling frequency of 250 Hz, i.e. 4715 snapshots have been acquired. The bulk velocity was simultaneously measured during the PIV measurements using the LDA.

GALA e.V., Karlsruhe, Germany, ISBN 978-3-9816764-6-4

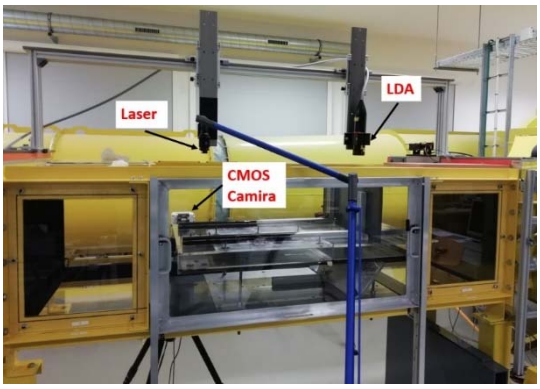

Fig. 4: PIV measurement experimental setup.

III- Pressure gradient measurements

Pressure gradients have been calculated from static pressure measurements using 16 pressure taps along the channel to establish the effect of the hexagonal structures on drag in the channel flow. All pressure measurement points were connected to pressure scanner (PSI 9116 Ethernet Pressure Scanner) provided with 16 channels for simultaneous pressure readings. For each test Reynolds number, the pressure gradient dp/dx was deduced by a linear regression of the measured pressure data. The location and dimensions of the pressure taps are given in fig.(5). At each streamwise position, there were three pressure taps installed (spanwise), prior to the final tests, to check the consistency of the readings as well as the two dimensionality of the flow. No static taps are located within the hexagonal structured test section as a precaution against any small flow disturbances introduced by the pressure taps to the flow over the hexagonal structured. A further reason was that studies on structures show that the presence of the structures greatly affects the static pressure in the flow field around it (Tay et al. 2015).

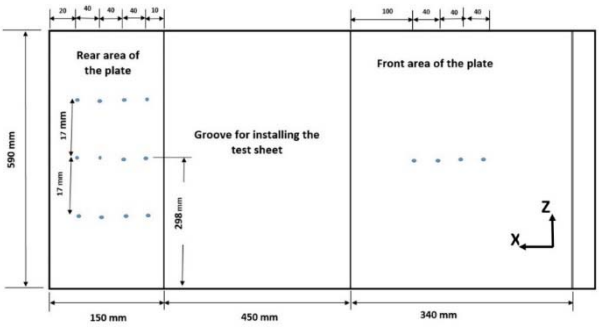

Fig. 5: Sketch for upper plate showing pressure taps locations.

Results

LDA measurements with a higher spatial resolution with $\Delta x \approx 0.14D$ and $\Delta z \approx 0.14D$ were carried out at $y/H = 0.05$ for Reynolds number of 10900, and the contours of the mean velocity normalized by the channel centerline velocity are shown in fig.(6) for channel heights 50 mm and 20 mm. The y coordinate has been measured from the flat surfaces between the hexagonal structures. The white lines show the position of the CS within the array.

As shown in fig.(6) that by the time the flow has reached the 11th row of structures, the mean stream wise velocity contours have reached an equilibrium state, and the flow for each structure are the same, regardless of their location in the array. This allows the study of a single structure in greater details and conclusions drawn from it are applicable for all the other structures in the array.

GALA e.V., Karlsruhe, Germany, ISBN 978-3-9816764-6-4

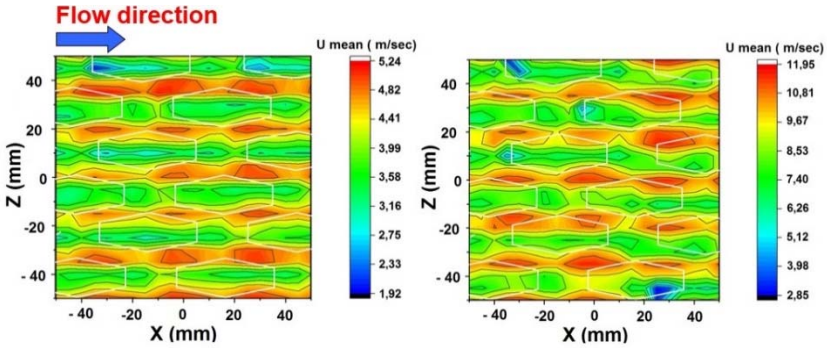

Fig. 6: Mean streamwise velocity contours for y/H = 0.05, Re = 10900, left channel height 50 mm and right channel height 20 mm.

I - Effect of the CS structures on the flow at different y/H

To study further the flow, measurements were taken at an even higher spatial resolution with $\Delta x \approx 0.07D$ and $\Delta z \approx 0.07D$ at four different heights with y/H = 0.05, 0.125, 0.25, and 0.5 at various Reynolds numbers. The contours of the mean velocity and the streamwise velocity fluctuations as shown in fig.(7) are also normalized by their respective values at the channel centerline (y/H = 0.5).

Close to the wall at y/H =0.05, the normalized mean streamwise contour showed two high velocity streaks lie on either side of the centerline over the CS. The contour patterns support the flow visualization results of (Ligrani et al. 2001, Won et al. 2005, Tay et al. 2015).

Tay et al. 2015 explained that the low and high-speed streaks are caused by the rotation of the vortices that bring the near-wall low speed fluid up from the centerline of the structure and the spanwise edges of the structure, and high velocity fluid from high above the wall downwards at the location of the high-speed streaks. This vertical movement of fluid is corroborated by the u_{rms} contours in fig.(7-bottom), where the low speed fluid originating from near the wall would show gr-eater fluctuations in the streamwise velocity than fluid from further up from the wall. By measuring away the wall at various y/H, the effect of the CS was minimized.

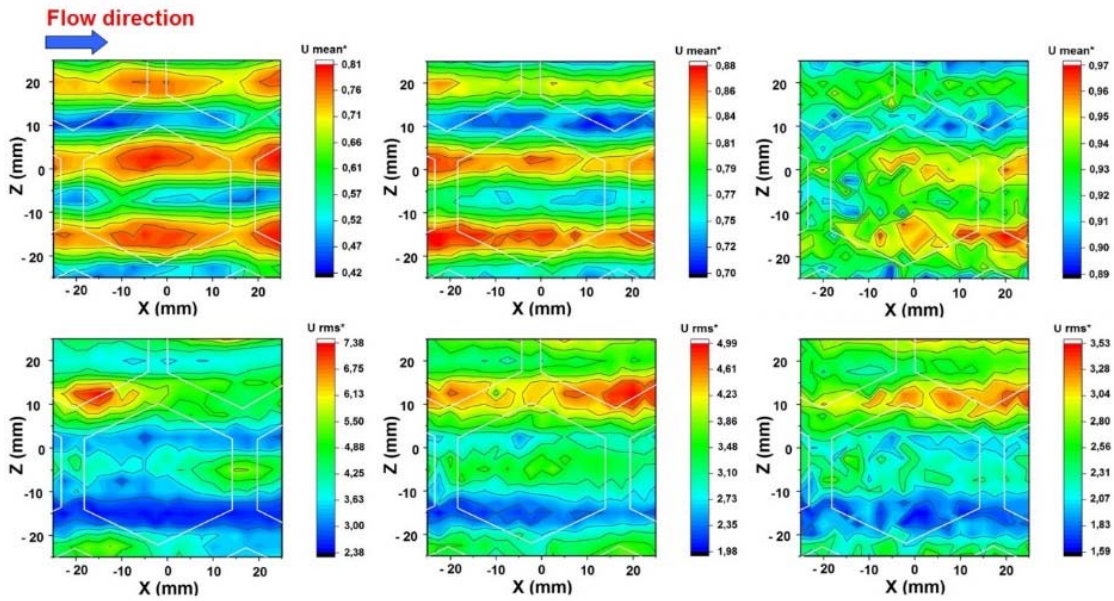

Fig. 7: Normalized mean streamwise (upper row) and fluctuation velocities (lower row) contours for Re = 10900 and channel height 50 mm at y/H = 0.05 (left), y/H = 0.125 (middle), and y/H = 0.25 (right). Mean streamwise and fluctuation velocities were normalized by their respective values at the channel centerline (y/H = 0.5).

GALA e.V., Karlsruhe, Germany, ISBN 978-3-9816764-6-4

II - Effect of the CS structures on the flow at different Re

As depicted in figure (8) for Re = 10900, the two high-speed streaks exists and visible in the contours for the other Reynolds numbers. Even more obvious are the changes in the u_{rms} contours in figure (8- bottom) as the Reynolds number increases.

At Re = 10900, the areas of high and low velocity fluctuations reflect the levels of fluctuations of where the fluid originated as the vortices bring up and down the local flow within the CS. As the Reynolds numbers increase, spanwise patterns develop within the contours. These spanwise patterns are expected for further develop and become more obvious as the Reynolds number increases.

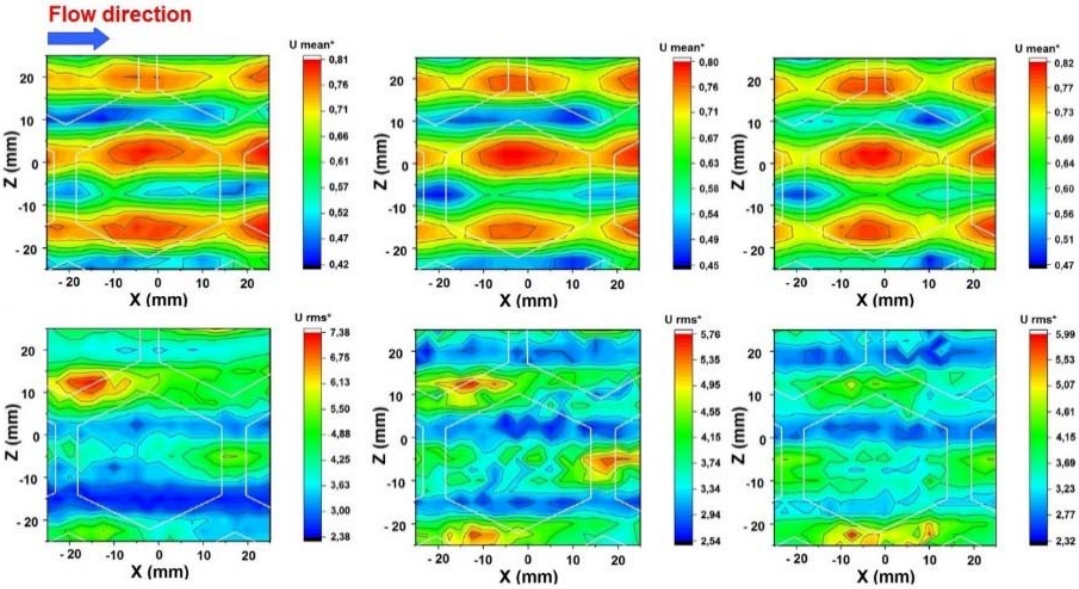

Fig. 8: Normalized mean streamwise (upper row) and fluctuation velocities (lower row) contours for y/H = 0.05 and channel height 50 mm at Re = 10900 (left), Re = 19100 (middle), and Re= 38000 (right). Mean streamwise and fluctuation velocities were normalized by their respective values at the channel centerline (y/H = 0.5).

III- Effect of the CS structures on the flow at different channel height (H)

Decreasing the channel height (H) from 50 mm to 20 mm did not affect the appearance of the two speed streaks as shown in fig.(9). Comparing fig.(8) with fig.(9) shows that the two speed streaks at H =20 have more strength compared to the contour of H =50 mm. This could be due to the rotation of the vortices are higher at H=20 that bring the near-wall low speed fluid up from the centerline of the structure and the spanwise edges of the structure, and high velocity fluid from high above the wall downwards at the location of the high-speed streaks.

In the other side, As the Reynolds numbers increase, spanwise patterns become weaker within the contours. Having weak spanwise patterns cause the normal cascading of the turbulent energy to the smaller scales for dissipation. This affect the drag and increase the skin friction.

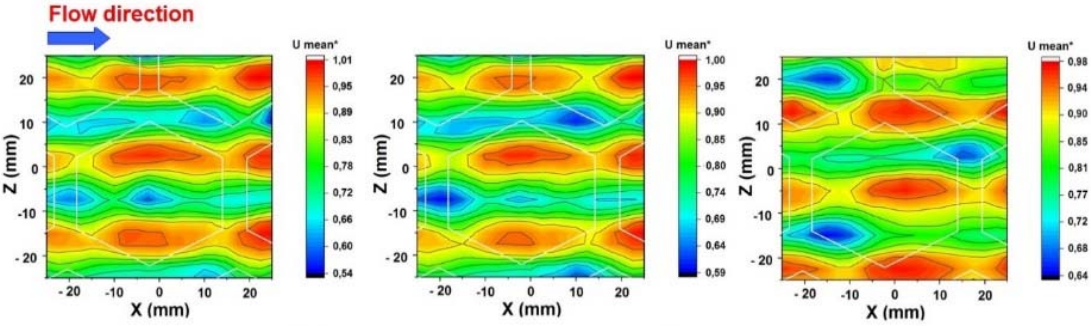

GALA e.V., Karlsruhe, Germany, ISBN 978-3-9816764-6-4

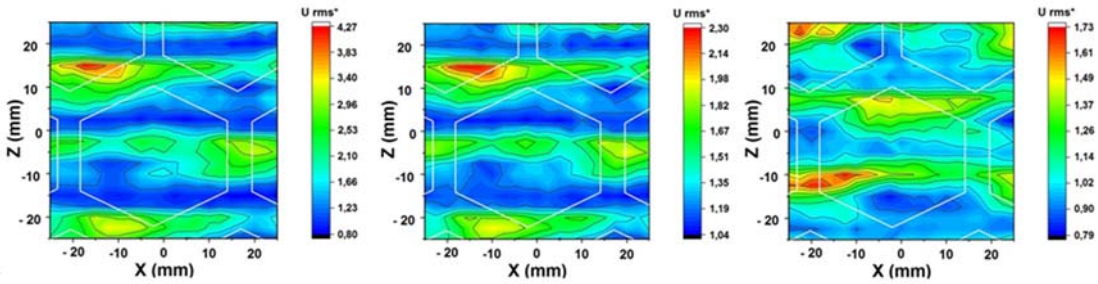

Fig.9 Normalized mean streamwise (upper row) and fluctuation velocities (lower row) contours for y/H = 0.05 and channel height 20 mm at Re = 7800 (left), Re = 10900 (middle), and Re= 12500 (right). Mean streamwise and fluctuation velocities were normalized by their respective values at the channel center-line (y/H = 0.5).

Skin friction Coefficient (C_f)

Based on the pressure gradient, the wall-shear stress T_w and the skin-friction coefficient C_f can be determined for the SPS and CS surfaces according to

$$T_w = -\frac{H}{2}\frac{dp}{dx} \quad , \quad C_f = \frac{Tw}{0{,}5\rho U^2}$$

Where ρ denotes the density of the fluid, dp/dx the pressure gradient along the channel.

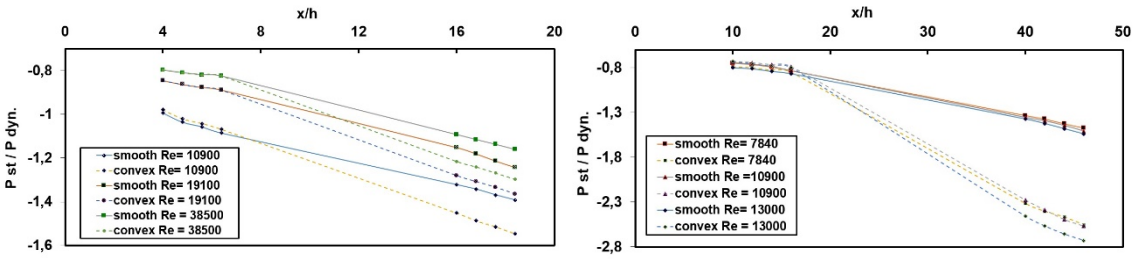

(a) (b)

Fig.10: Pressure losses measured along the upper plate of the channel for both SPS and CS normalized by dynamic pressure at inflow at (a)H/k =6.4 and (b) H/k =16.1.

Table (1): Calculations of the C_f for SPS and CS surfaces at different channel heights and Reylonds numbers.

H (mm)	Re	Surface	T_w (kg/m sec^2)	C_f	
50	10900	Smooth	0,0006575	2,59369E-05	49,43%
		Convex	0,0009825	3,87574E-05	
	19100	Smooth	0,00065	1,88079E-06	40,38%
		Convex	0,0006575	2,64034E-06	
	38000	Smooth	0,0009125	7,92824E-06	36,86%
		Convex	0,0009375	1,08507E-05	
20	7800	Smooth	0,00041	4,74537E-06	169,76%
		Convex	0,001106	1,28009E-05	
	10900	Smooth	0,00043	2,68091E-06	147,91%
		Convex	0,001066	6,64615E-06	
	13000	Smooth	0,000416	1,73333E-06	190,87%
		Convex	0,00121	5,04167E-06	

As depicted in table (1), the pressure gradient measurements shows a dramatic increase in the skin friction of the CS surface compared to the SPS.

PIV measurement

A preliminary analysis was done for the PIV measurements that carried out for channel height 50 and 20 mm. The measurements have been occurred rear the tested sheets. The size of the images was chosen to be 1686×1227 pixels and the sampling frequency was set at 250 Hz. Particle images were analyzed by employing the iterative multi-pass decreasing size

GALA e.V., Karlsruhe, Germany, ISBN 978-3-9816764-6-4

method. The window size in the final iterative step is 32×32 pixels after three times of iterations. A selected sample of the instantaneous velocity field is presented in fig.(11) for Re = 10900 and channel heights 50 for the SPS and CS. The CS shows regions of stream wise velocity fluctuations are observable in the core region of flow field that might be considered as a sign of the large-scale motion in the structured channel flow. Further, these measurements will be discussed in a separate publication.

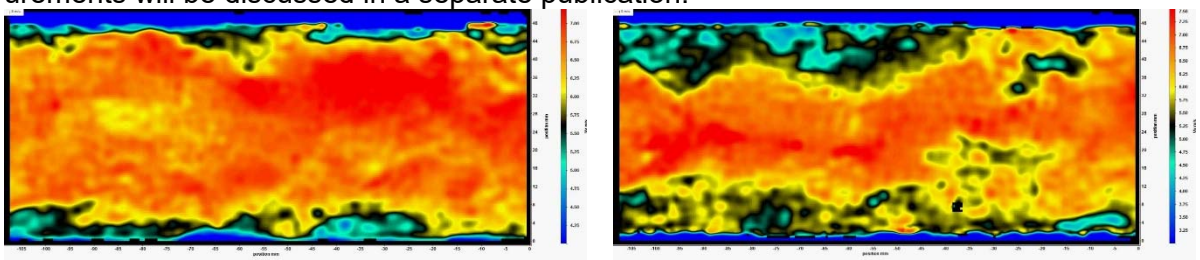

(a) (b)

Fig.11: PIV instantaneous velocity field Re = 10900 and H= 50 mm (a) Smooth surface and (b) Convex surface.

Conclusion

An experimental investigation has been carried out over hexagonal convex structured cavity inside fully turbulent channel flow. Different measurement techniques (LDA, PIV and pressure gradient measurements) have been conducted at two different channel height to study the behavior of the flow over the hexagonal structured cavity.

The present study showed that the CS cavity introduces streamwise vorticity into the basic flow. The streamwise vorcity appears as two high velocity streaks lie on either side of the centerline of the hexagonal cavity and start to vanish as the y/H increase until they disappear completely at the center of the channel. This behaviour agrees with the behaviour of the flow over dimples as reported by (Ligrani et al. 2001, Won et al.2005, Tay et al. 2015 and concave hexagonal structured Yousry et al. 2017).

Examining the CS at different Re numbers (10900, 19100, and 38000) as shown in fig.(7), that the flow near the wall (y/H= 0,05) got areas of high and low velocity fluctuations reflect the levels of fluctuations of where the fluid originated as the vortices bring up and down the local flow within the CS. As the Reynolds numbers increase, spanwise patterns develop within the contours. These spanwise patterns are expected for further develop and become more obvious as the Reynolds number increases.

In addition, we investigate the influence of the CS on the flow at different channel heights. Changing the channel height did not affect the appearance of the two speed streaks as shown in fig.(8). Our hypothesis is that rotation of the vortices are higher at lower channel height that bring the near-wall low speed fluid up from the centerline of the structure and the spanwise edges of the structure, and high velocity fluid from high above the wall downwards at the location of the high-speed streaks. In the other hand, increasing the Re affect spanwise patterns and became weaker. Having weak spanwise patterns lead to increase the local skin friction. The pressure gradient measurements shows dramatic increase in the total skin friction of the CS compared to the SPS as shown in table (1).

Finally, an analysis has been performed for the PIV measurements that carried out for channel height 50 and 20 mm. The instantaneous velocity field showed that the CS got regions of streamwise velocity fluctuations are observable in the core region of flow field that might be considered as a sign of the large-scale motion in the structured channel flow.

GALA e.V., Karlsruhe, Germany, ISBN 978-3-9816764-6-4

Acknowledgement

I would like to thank the BTU Graduate Research School (GRS) for financing the research.

References

C. M. J. Tay, Y.T. Chew, B.C. Khoo, J.B. Zhao, 2014:''Development of flow structures over dimples'', Experimental Thermal and Fluid Science. 52, 278–287.

C. M. J. Tay, B. C. Khoo, and Y. T. Chew, **2015**: ''Mechanics of drag reduction by shallow dimples in channel flow'', Physics of fluids. 27, 035109.

G. I. Mahmood and P. M. Ligrani, **2002**:''Heat transfer in a dimpled channel: Combined influences of aspect ratio, temperature ratio, Reynolds number, and flow structure'', Int. J. Heat Mass Transfer. 45, 2011–2020.

G. V. Kovalenko, V. I. Terekhov, and A. A. Khalatov, 2010: ''Flow regimes in a single dimple on the channel surface'', J. Appl. Mech. Tech. Phys. 51, 839–848.

H. G. Kwon, S. D. Hwang, and H. H. Cho, 2011: ''Measurement of local heat/mass transfer coefficients on a dimple using naphthalene sublimation'', Int. J. Heat Mass Transfer. 54, 1071–1080.

I. Marusic, B. J. McKeon,P. A. Monkewitz, H. M. Nagib, A. J. Smits,and K. R. Sreenivasan, 2010 : '' Wall bounded turbulent flow at high Reynolds number: Recent advances and key issues'', Physics of fluids. 22, 065103.

M. Yousry, S. Merbold, C. Egbers, 2017: '' LDA measurements over hexagonal structured cavity inside turbulent channel flow'', German Association for Laser Anemometry GALA e.V. ISBN 978-3-9816764-3-3.

N. K. Burgess and P. M. Ligrani, 2005: ''Effects of dimple depth on channel Nusselt numbers and friction factors'', J. Heat Transfer. 127(8), 839–847.

P. M. Ligrani, N. Burgess, and S. Y. Won, 2005: ''Nusselt numbers and flow structure on and above a shallow dimpled surface within a channel including effects of inlet turbulence intensity level'', J. Turbomach. 127, 321–330.

P. M. Ligrani, J. L. Harrison, G. I. Mahmood, and M. L. Hill, 2001: '' Flow structure due to dimple depression on a channel surface'', Phys. Fluids. 13(11), 3442–3451.

S. A. Isaev, A. I. Leontiev, N. A. Kudryavtsev, and I. A. Pyshnyi, 2003: '' The effect of rearrangement of the vortex structure on heat transfer under conditions of increasing depth of a spherical dimple on the wall of a narrow channel'', High Temperature 41(2), 229–232.

S. A. Isaev, N. V. Kornev, A. I. Leontiev, and E. Hassel, 2010: '' Influence of the Reynolds number and the spherical dimple depth on turbulent heat transfer and hydraulic loss in a narrow channel'' Int. J. Heat Mass Transfer. 53, 178–197.

S.Merbold, 2009: ''Zum strömungsphysikalischen Einfluss strukturierter Vertiefungen auf den Reibungswiderstand von turbulent überströmten Oberflächen'' Diploma thesis , Georg-August-University Göttingen.

S.Y.Won, Q. Zhang, and P. M. Ligrani, 2005: ''Comparisons of flow structure above dimpled surfaces with different dimple depths in a channel'', Phys. Fluids 17, 045105.

U. Butt, Ch. Egbers, 2013. Aerodynamic characteristics of flow over circular cylinders with patterned surface'', Int. Journal of Materials, Mechanics and Manufacturing.1, Nr. 2, 121-125.

U. Butt, 2014:''Experimental investigation of the flow over macroscopic hexagonal structured surface'', Doctoral thesis.

U. Butt, C. Egbers, 2016: ''Flow structure due to hexagonal cavities and bumps on a plate surface", Thermophysics and Aeromechanics.

V.V. Alekseev, I. A. Gachechiladze, G. I. Kiknadze, and V. G. Oleinikov, 1998: '' Tornado-like energy transfer on three-dimensional concavities of reliefs-structure of self-organizing flow, their visualisation, and surface streamlining mechanisms'', in Transactions of the 2nd Russian National Conference of Heat Transfer, Heat Transfer Intensification Radiation and Complex Heat Transfer (Publishing House of Moscow Energy Institute (MEI). 6, pp. 33–42.

Z. Y. Wang, K. S. Yeo, and B. C. Khoo, 2006: '' DNS of low Reynolds number turbulent flows in dimpled channels'', J. Turbul. 7, N37.